J. Braz. Chem. Soc., Vol. 20, No. 7, 1327-1333, 2009.
Printed in Brazil - ©2009 Sociedade Brasileira de Química
0103 - 5053 $6.00+0.00

Article

A New Polyacetylene from *Vernonia scorpioides* (Lam.) Pers. (Asteraceae) and its *in vitro* Antitumoral Activity

Humberto Buskuhl,[a] Rilton A. Freitas,[a] Franco Delle Monache,[b] Andersson Barison,[c] Francinete R. Campos,[c] Yuri E. Corilo,[d] Marcos N. Eberlin[d] and Maique W. Biavatti*[,a,#]

[a]*Centro de Ciências da Saúde, Universidade do Vale do Itajaí, 88302-202 Itajaí-SC, Brazil*

[b]*Dipartimento di Chimica e Tecnologia delle Sostanze Biologicamente Attive, Università "La Sapienza", Roma, Italy*

[c]*Departamento de Química, Centro Politécnico, Universidade Federal do Paraná, 81530-900 Curitiba-PR, Brazil*

[d]*Instituto de Química, Universidade Estadual de Campinas, 13083-970 Campinas-SP, Brazil*

A fração diclorometano obtida pelo particionamento do extrato hidroalcoólico obtido das folhas e flores de *Vernonia scorpioides* (Asteraceae) resultou no isolamento e caracterização de um novo poliacetileno, 5-octa-2,4,6-triinil-furan-2(5H)-ona. A determinação estrutural foi baseada em dados de espectrometria de Ressonância Magnética Nuclear mono e bidimensionais, de Massas e de Infravermelho. Foi investigado o potencial antitumoral e genotóxico do novo poliacetileno e os resultados encontrados sugerem genotoxicidade e citotoxicidade, onde a morte celular ocorreu *via* apoptose, envolvendo um mecanismo dependente de caspase.

The dichloromethane fraction obtained from hydroalcoholic crude extract of leaves and flowers of *Vernonia scorpioides* (Asteraceae) was investigated, resulting in the isolation and structure elucidation of a new polyacetylene namely 5-octa-2,4,6-triynyl-furan-2(5H)-one. The structure of the isolated compound was determined based on IR, NMR (1D and 2D) and MS spectrometric data. The antitumor potential, including cytotoxicity to tumor cells and genotoxicity, was investigated. The results suggest that apoptotic cell death may have occurred, at least in part, *via* a caspase-dependent mechanism.

Keywords: polyacetylene, *Vernonia scorpioides*, cytotoxicity, genotoxicity, Asteraceae

Introduction

The widespread genus *Vernonia* (Asteraceae) is characterized by the fact that it produces highly oxygenated sesquiterpene lactones, such as glaucolides and hirsutinolides, some of which are allenic lactones. Many other compounds have also been isolated, such as thiophenes and dithio compounds.[1,2] Among the species of *Vernonia*, cytotoxicity has been described for isolated sesquiterpene lactones from *V. cinerea*,[3] *V. lasiopus*,[4] and *V. amygdalina*.[5] Besides sesquiterpene lactones, polar compounds from water-soluble extracts of *Vernonia* have also been found to have cytotoxic and imunomodulatory activities such as those from the edible leaves of *V. amygdalina*[6] and from the roots of *V. kotschyana*[7] and *V. anthelmintica*.[8]

The species *Vernonia scorpioides* (Lam.) Pers., which is very common in Brazil, is popularly known as "Piracá", "Enxuga" or "Erva-de-São-Simão" and usually grows in poor deforested neotropical soils.[9] Alcoholic extract from the fresh leaves is widely used in topical applications, to treat a variety of skin disorders, including chronic wounds, such as ulcers of the lower limbs. In previous studies, chloroform and hexane crude extracts of *V. scorpioides* leaves have shown fungicide activity,[10] moderate bactericide activity and mild wound healing effects.[11] In addition, in mice treated with dichloromethane extract of the leaves, the Ehrlich tumor disappeared completely.[12] Therefore, as part of our ongoing search for bioactive compounds of *V. scorpioides*, a new polyacetylene isolated from the dichloromethane fraction is described, and its antitumor potential, as well as *in vitro* cytotoxicity to tumor cells and cell death *via* genotoxicity, are evaluated.

*e-mail: maique@ccs.ufsc.br
[#] Present address: Laboratório de Farmacognosia, Departamento de Ciências Farmacêuticas, Centro de Ciências da Saúde, Universidade Federal de Santa Catarina, Trindade, 88040-900 Florianopolis-SC, Brazil

Results and Discussion

The crude ethanol extract of *V. scorpioides* was successively partitioned with hexane, dichloromethane and ethyl acetate. Successive chromatographic separations of dichloromethane fraction as described in the Experimental section resulted in the isolation of a new polyacetylene (**1**).

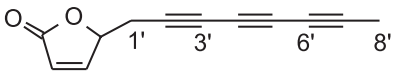

Polyacetylene **1** was obtained in the form of colorless crystals with the molecular formula $C_{12}H_8O_2$, as deduced from its HR-TOF-MS (observed *m/z* 185.0597 $[M + H]^+$) and NMR data. Additionally, the ESI-MS/MS (25%) experiment of deprotonated molecule **1** gave a predominant ion product at *m/z* 139 $[(M - H - 44)^-]$, corresponding to the loss of carbon dioxide, suggesting the presence of a lactone carbonyl group. The IR spectrum exhibited strong absorption bands at 1289 and 1786 cm^{-1}, which were attributed to the α,β-unsaturated five member conjugated lactone, supported by a ^{13}C NMR chemical shift at 171.9 ppm. On the other hand, the expected alkyne stretching in the 2100-2250 cm^{-1} range was not observed. This is because the internal alkynes had very small bond dipole moments and as a result, symmetrical alkynes showed little or no absorption. The UV spectrum revealed only one band at 207 nm. The ^1H NMR spectrum showed only two spin systems, one containing an isolated methyl group (δ 1.97 *s*, H-8') and the other consisting of one methyne [δ 5.14 *dddd* (7.9, 5.2, 1.9 and 1.5 Hz), H-5], one methylene [δ 2.95 *dd* (17.4 and 5.2 Hz), H-1'a and 2.67 *dd* (17.4 and 7.9 Hz), H-1'b] and two olefinic hydrogens [δ 6.23 *dd* (5.7 and 1.9 Hz), H-3 and 7.56 *dd* (5.7 and 1.5 Hz), H-4], (Table 1). The ^{13}C NMR data, together with one-bond ^1H-^{13}C correlations in the HSQC experiment of **1,** indicated the presence of 12 carbons, comprising seven quaternary, being one at 171.9 ppm, attributed to a conjugated carbonyl group, and further six in the 76.2 to 58.7 range, as well as one methyl, one methyne, one methylene and two olefin (Table 1). Both olefin hydrogens at δ 7.56 and 6.23 showed long-range ^1H-^{13}C correlations in the HMBC experiment with carbon at δ 171.9, confirming the α-β-unsaturated lactone system, as well as with methyne carbon at 79.6 ppm, evidencing a five-member lactone ring. Additionally, methyne hydrogen at 5.14 ppm showed correlations with methylene carbon at 24.5 ppm, which is attached to the lactone ring, as evidenced in the ^1H NMR spectrum. Furthermore, ^1H-^{13}C long-range correlation of methylene hydrogens H-1' with carbons C-2', C-3', C-4' and C-5', as well as those of the methyl hydrogens H-8' with carbons C-7', C-6', C-5' and C-4', enabled us to identify the polyacetylene system and the unequivocal ^{13}C NMR chemical shift assignments of carbons C-2' to C-7' (Table 1). The low ^{13}C NMR chemical shift at 4.5 ppm observed for methyl group C-8' is due to high shielding effect of the triple bonds. Therefore, polyacetylene **1** is named as 5-octa-2,4,6-triynyl-furan-2(5H)-one, which was compared with previously published polyine signals.[13-16]

Table 1. NMR spectroscopy data for the polyacetylene **1**[a]

Position	δ_C, mult.	δ_H, mult. (*J* in Hz)	HMBC ^1H-^{13}C [b]
2	171.9, C		
3	122.9, CH	6.23, *dd* (5.7; 1.9)	2, 4, and 5
4	154.5, CH	7.56, *dd* (5.7; 1.5)	2, 3, and 5
5	79.6, CH	5.14, *dddd* (7.9; 5.2; 1.9; 1.5)	3, 4, 1' and 2'
1'	24.5, CH_2	a 2.95, *dd* (17.4; 5.2) b 2.67, *dd* (17.4; 7.9)	4, 5, 2', 3', 4', 5' and 6' 4, 5, 2', 3', 4', 5' and 6'
2'	70.5, C		
3'	69.3, C		
4'	58.7, C		
5'	62.3, C		
6'	64.6, C		
7'	76.2, C		
8'	4.5, CH_3	1.97, *s*	2', 3', 4', 5', 6' and 7'

[a]The experiments were taken at 293 K at 400.13 and 100.61 MHz for ^1H and ^{13}C, respectively in $CDCl_3$ and TMS as internal reference (δ 0.00). [b]Long-range ^1H-^{13}C HMBC correlations, optimized for 8 Hz, are from hydrogen(s) stated to the indicated carbon.

More than 750 naturally occurring polyacetylene derivatives belong predominantly to the family Asteraceae, subtribe Heliantheae. They are also present in several other plant families (Apiaceae, Araliaceae), as well as certain basidiomycete fungi. Straight chain polyacetylenes are the most common, while thiophenes and thiarubrines, sulphur heterocycles produced from polyacetylenes, are not widely distributed.[17] However, the occurrence of a polyacetylene in the genus *Vernonia* is described for the first time in this work.

Polyacetylenes have been attracting attention due to their wide spectrum of biological activities, such as plant growth inhibition[18,19] and their antifungal,[20-22] antibacterial[17,23] and insecticidal activities,[24] indicating an important role in the protection and developmental physiology of the plant. Moreover, polyacetylenes have been proven to be cytotoxic against some cancer cell lines.[25,26]

The polyacetylene **1** cytotoxicity was investigated using MTT assay on two tumor cells (B16F10 and HeLa) and one non-tumor (L929) cell. Succinate-dehydrogenase, a mitochondrial enzyme which is present in living cells, cleaves the tetrazolium ring, converting the MTT to an insoluble purple formazan.[27] Significant cytotoxicity

was observed for the HeLa tumor cells with an IC_{50} of 158.1 μmol L^{-1} after 24 h treatment, showing a reduction of 41% in growth of HeLa tumor cells with the application of 543 μmol L^{-1} ($P < 0.001$) of polyacetylene **1** (Figure 1C). On the other hand, the L929 non-tumor cells were resistant to exposure to polyacetylene **1** at the tested concentrations (Figure 1A). However, no significant difference in cytotoxic effect was observed between the B16F10 tumor and L929 non-tumor cells, indicating specific cytotoxicity for HeLa tumor cells (Figure 1).

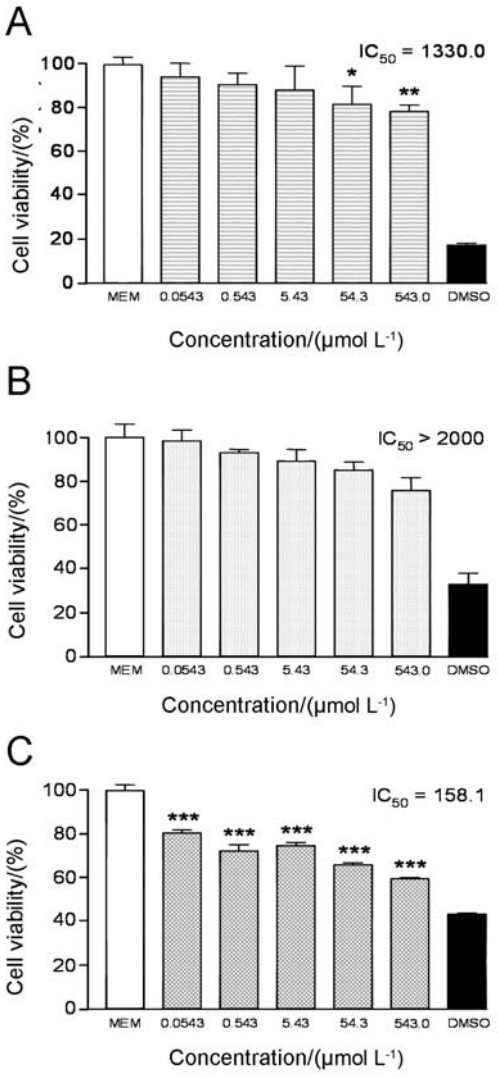

Figure 1. Cytotoxicity effect of polyacetylene 1 in L929 (A) B16F10 (B) and HeLa (C) cells for 24 hours. MEM and DMSO were used as negative and positive control, respectively. Bars represent mean values ± SD. *p < 0.05 **p < 0.01 ***p < 0.001 ANOVA followed by Tukey.

However, significant cytotoxicity was observed for the L929 non-tumor cells after just one-hour of treatment with polyacetylene **1** (IC_{50} 55.3 μmol L^{-1}) (Figure 2A). Therefore, the necrotic cell death of the L929 non-tumor cells was evaluated after 1 hour, by lactate dehydrogenase (LDH) assay, with lower LDH activity (525 ± 44 U/l) being observed in the presence of polyacetylene **1** compared with the positive control (2585 ± 114 U/l) (Figure 2B), indicating non-specific cell death, associated with necrosis, for L929 cells in short contact. After an initial period of stress, probably generated by the necrosis, the remaining cells began a new proliferative cycle, reducing their cytotoxicity levels (IC_{50} 1130 μmol L^{-1} after 24 h).

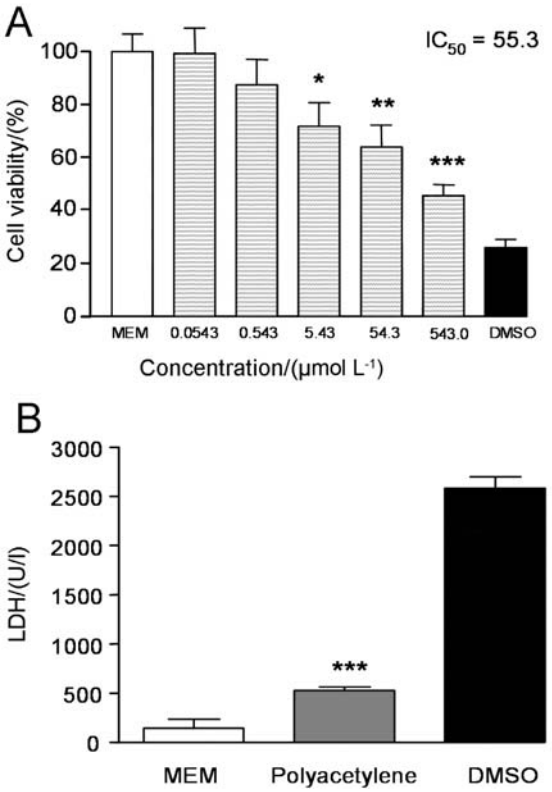

Figure 2. L929 cell viability (A) and LDH release (B) in L929 cells after 1 hour of incubation in the presence of polyacetylene **1**. MEM and DMSO were used as negative and positive control, respectively. Bars represents mean values ± SD. *p < 0.05 **p < 0.01 ***p < 0.001 ANOVA followed by TUKEY.

In order, to evaluate other mechanisms related to the cytotoxicity of polyacetylene **1**, apoptotic changes in the L929 non-tumor cells were verified. After 24 h in the presence of polyacetylene **1**, only 22.7% of the cells showed ethidium bromide staining, while the remaining 77.3% cells showed staining only using Annexin V-FITC, indicating early apoptotic stages. On the other hand, the positive control (DMSO) showed extensive ethidium bromide staining, indicating necrotic action. The same approach was adopted for the B16F10 and HeLa tumor cells. In these cases, the necrotic cells were evidenced by the presence of an intact cell nucleus stained with ethidium bromide, as well as apoptotic cells, identified by nuclear fragmentation and apoptotic bodies and cells with cytoskeletal alterations,

which were observed by using Annexin V-FITC. As a result, this analysis revealed an association of necrotic and apoptotic processes. However, the cells stained with ethidium bromide comprised less than 25% of the total, indicating a predominant apoptotic process. Therefore, caspase-3 activity in B16F10 and HeLa tumor cells, after 24 h of incubation, was also evaluated as an indicator of apoptosis induction, since different upstream pathways leading to apoptosis depend on caspase-3 induction for final apoptotic execution. Figure 3 shows the effect of polyacetylene **1**, at the level of caspase-3 induction. There was no significant increase in caspase-3 activity in either group of cells at 1 μmol L^{-1}, when compared with negative control (Figure 3). A slight increase in caspase-3 activity was observed at 5 μmol L^{-1}, and a twofold increase at 10 μmol L^{-1}. These results are in agreement with those obtained by Choi *et al*.[28] in their studies of caspase-3 and 9 activities using the same approach and concentrations (5 and 10 μmol L^{-1}) of test compound. Caspases belong to the family of proteins that play a key role in the execution of apoptosis, and are responsible for many of the morphological features normally associated with this form of cell death.[29] Isoforms 3 and 7 are the main caspases family members involved in the induction and execution of the programmed cell death process.[28,29] Therefore, caspase-3 activation is essential for DNA fragmentation to occur in apoptosis induced by a variety of stimuli. In line with these observations, our experiments clearly demonstrate that apoptotic cell death might account, at least in part, for the antitumor activity of polyacetylene **1**. Notably, the data in the present study suggest that apoptotic cell death may be occurring, at least in part, *via* a caspase-dependent mechanism. To confirm the occurrence of apoptosis induced by polyacetylene **1**, nuclear damage to DNA was assessed by comet assay using medulla cells. Negative control was performed with DMSO, which causes cell membrane disruption, with low DNA genotoxicity, while methyl methanesulfonate (MMS) at 40 μmol L^{-1} was used as positive control, which is responsible for alkylation of DNA and extensive genotoxicity. The assay indicated a genotoxic distribution of polyacetylene at 54.3 μmol L^{-1} in levels 1-4, mainly in level 3 (see Experimental section). By contrast, the negative control showed this distribution in levels 0-1, while the positive control showed a damage index in levels 3-4, particularly the latter. The damage index determination show a significant genotoxicity of polyacetylene **1**, which was 49% higher than the negative control, and only 20% lower than the positive control (Figure 4). It is speculated that the extensive genotoxicity could explain the activation of apoptosis, due to extensive damage to the DNA, and the induction of apoptosis through p53 activation, or else the apoptosis activated the caspase-3 apoptotic enzyme, followed by DNA fragmentation, or even both events occurring at the same time. In previous unpublished results, polyacetylene **1** induced DNA fragmentation, observed by DNA gel electrophoresis, with an association of unspecified genotoxicity and a ladder-like pattern, which is a typical character of DNA cleavage between nucleosomes, indicating DNA apoptosis profile damage for HeLa cells. Non-polar polyacetylene **1** showed genotoxic activity, and its hydrophobicity could be one reason for this behavior, due to its high capacity to cross the cell and nuclear membranes. In future studies, some chemical modification of polyacetylene **1** could be planned, generating a less toxic compound, reducing the unspecific die by necrosis or genotoxicity, and increasing the process of apoptosis.

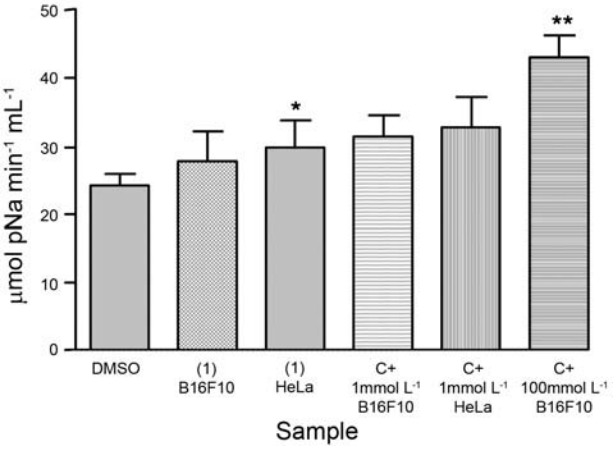

Figure 3. Caspase-3 (μmol pNa min^{-1} mL^{-1}) activity in HeLa and B16F10, after 24 h of exposure to polyacetylene **1**. DMSO was used as negative control, while paclitaxel (C+) at 1 and 100 mmol L^{-1} were used as positive control. Bars represent Mean ± SD. *p < 0.05 **p < 0.01 ANOVA followed by Tukey.

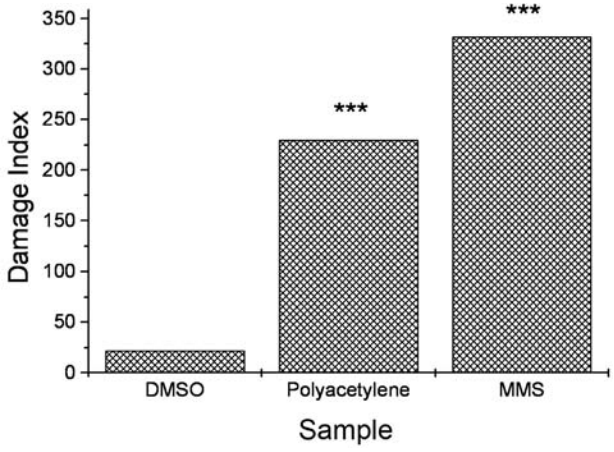

Figure 4. Damage index in the bone marrow cells after 1 hour of exposure of polyacetylene **1** at 54.3 μmol L^{-1}. DMSO was the negative control, while MMS at 40 μmol L^{-1} was the positive control. ***p < 0.001 ANOVA followed by Tukey.

Experimental

General procedures

The melting point was determined using a QUIMIS Q-340S23 micromelting point apparatus. The UV spectrum was obtained in MeOH using a Shimadzu UV-Vis 2401PC spectrophotometer. The IR spectrum was measured in KBr pellets using a Bomen Hartmann & Braun B-100 spectrophotometer. All the NMR data were recorded at 293 K in $CDCl_3$ using a Bruker AVANCE 400 spectrometer operating at 9.4 T, observing ^1H and ^{13}C at 400.13 and 100.61 MHz, respectively.

^1H-^{13}C correlation (HSQC and HMBC) experiments were optimized for an average coupling constant ^1J(C,H) of 140 Hz and ^{LR}J(C,H) of 8 Hz, respectively. All the NMR chemical shifts (δ) were given ppm related to TMS as internal reference (0.00 ppm), and all the pulse programs were supplied by Bruker. Low-resolution ESI-MS and ESI-MS/MS data were acquired in the negative ion mode, using a Bruker Esquire 6000 ESI-ion trap instrument, while the high-resolution HR-TOF-MS measurement was carried out using a hybrid quadrupole reflector orthogonal time-of-flight high resolution Micromass Q-TOF mass spectrometer, equipped with an electrospray source.

Plant material

Flowers and leaves of *Vernonia scorpioides* were collected from wild specimens of "restinga" forest (a distinct type of coastal tropical and subtropical moist broadleaf forest) in Navegantes in November 2006 and identified by Dr. Ana Claudia Araújo, of the Universidade do Vale do Itajaí (UNIVALI). A voucher specimen (M. Biavatti 11) was deposited at the Barbosa Rodrigues Herbarium (HBR), Itajaí, Santa Catarina, Brazil.

Extraction and isolation

Fresh flowers and leaves of *Vernonia scorpioides* (3 kg) were extracted with ethanol (6 L) at room temperature, in absence of light, for seven days. After solvent reduction to 1/6 of initial volume under reduced pressure and the addiction of water (500 mL), the extract was submitted to liquid-liquid fractioning using solvents with increasing polarities, to give *n*-hexane (1.2 g), dichloromethane (2.3 g), and ethyl acetate (1.4 g) fractions. The dichloromethane fraction was initially subjected to silica gel column chromatography (CC) (60-230 mesh) eluted with *n*-hexane (500 mL), followed by dichloromethane (800 mL), ethyl acetate (700 mL) and methanol (400 mL), yielding one subfraction for each of the four solvents. Additional chromatography separation of the dichloromethane subfraction (420 mg) by silica gel CC (230-400 mesh), using *n*-hexane with increasing concentrations of ethyl acetate (0-50%) as eluent, and collecting eluate portions of 30 to 50 mL each (47 flasks), resulted in polyacetylene **1** (6 mg, flasks 6, 7 and 8).

*5-Octa-2,4,6-triynyl-furan-2(5H)-one (**1**)*

Colorless crystals ($CHCl_3$), mp 98-100 °C; UV (MeOH) λ_{max}/nm: (log $\in$) 207 (5.58); IR (KBr) ν_{max}/cm^{-1}: 3081, 2515, 2438, 1786, 1289, 791, 679, 631, 551, 329; ^1H and ^{13}C NMR data shown in Table 1; ESI-MS *m/z* 183.0 $[M - H]^-$; ESI-MS/MS (daughter ions, 25%) *m/z* 139 $[M - H - CO_2]^-$ (100), 87 (3); HR-TOF-MS (ESI positive) *m/z* 185.0597 $[M + H]^+$ (calc. for $C_{12}H_8O_2 + H^+$, 185.0603).

Cells and cell culture conditions

The fibroblast L929 (*Mus musculus* C3H/NA) (BCRJ CR020/ATCC CCL1), B16F10 melanoma (*Mus musculus* C57BL/6J) (BCRJ CR010), and HeLa from cervix adenocarcinoma *(Homo sapiens)* (BCRJ CR050) were obtained from the Cell Bank of Rio de Janeiro (BCRJ), Brazil. The cells were maintained in minimal essential medium (MEM) supplemented with 0.2% sodium bicarbonate (Invitrogen/GIBCO), 10% heat inactivated fetal calf serum (FCS), 1% non-essential aminoacids (Invitrogen/GIBCO), two mmol L^{-1} L-glutamine, and antibiotic PCN 0.1% (Invitrogen/GIBCO). The cells were maintained in a fully humidified atmosphere (95% air, 5% CO_2) at 37 °C. Cell viability was analyzed before each assay by trypan blue dye exclusion assay, which was always greater than 98%. For the damage index, (Comet assay) bone marrow cells were obtained from femur bones of *Mus musculus*, (Swiss). The ethical animal research committee of UNIVALI approved the protocol (# 236/07). The cells were obtained after vivisection using an O_2/CO_2 chamber, and the femur was obtained by surgery. Cell viability was analyzed before each assay, by trypan blue dye exclusion assay, which was always greater than 95%.

Cytotoxicity assay

Cell viability was determined using the cell proliferation reagent MTT (3-[4,5-dimethylthiazol-2-yl]-2,5-diphenyltetrazolium bromide) a tetrazolium salt that is cleaved by mitochondrial dehydrogenages in viable cells.[27] 100 µL Containing 2×10^4 of cell suspension was placed briefly in each of 96-well plates. Next, cell cultures were treated with the polyacetylene **1** at concentrations

of 0.0543, 0.543, 5.43, 54.3, 543.0 μmol L^{-1}. After one and 24 h incubation, 20 μL of the proliferation reagent MTT at concentration of 5 mg mL^{-1} in phosphate-buffered saline (PBS, pH 7.4) was added to each well and the cells were incubated at 37 °C for 4 h in humidified atmosphere with 5% CO_2. Formazan precipitates were solubilized by addition of 100 μL of DMSO. After 10 min at room temperature, spectrophotometric absorbance at 570 nm of each well was measured on a microculture plate reader. Cell viability percentage was calculated as [1-(absorbance of experimental wells/absorbance of control wells) × 100].

Lactate dehydrogenase assay

Lactate dehydrogenase (LDH) is a stable cytosolic enzyme that is released upon membrane damage and was used as an index of cytotoxicity. The LDH activity was measured using a commercial cytotoxicity assay kit (DiaSys). L929 cells containing 5×10^5 of cell suspension were placed in each of 6-well plates and incubated at 37 °C for 1 hour in a humidified atmosphere with 5% CO_2, in the presence of polyacetylene **1**.[30] Maximal LDH release of the cells was determined by addition of lysis solution (0.8% Triton X-100), followed by incubation at 37 °C for 45 min. Absorbance at 360 nm was determined photometrically and activity was represented as ΔA/min × 2000 (U/I). LDH activity released by cells cultured in absence or presence of polyacetylene **1**, was compared with the negative control.

Detection of apoptosis

Apoptotic changes in L929, B16F10, and HeLa cells were evaluated using the Annexin V-FITC/ethidium bromide apoptosis detection kit. Cells culture containing 2×10^4 of cell suspension in each well plate was cultured in the presence of polyacetylene **1** for 24 h. Determination of phosphatidylserine externalization was followed by *in situ* detection protocols. Briefly, after 24 h treatment, the cells were washed with cold PBS and incubated in 100 μL of MEM, containing 1 μL of annexin V-FITC (12 mg mL^{-1}) and 50 μL of ethidium bromide (2 μg mL^{-1}) at room temperature for 15 min in the dark. The cells were evaluated using an Olympus CKX41SF2 microscope, a CKX41-RFA fluorescence system, and an Olympus Q-color3 system equipped with 480 and 520 nm filters.[30]

Caspase-3 activity assay

Caspase-3 activity was measured in cell lysates using a SIGMA caspase-3 assay Kit, according to the manufacturer's protocols. Briefly, HeLa and B16F10 cells were cultured for 24 h (37 °C, 5% CO_2) in the presence of polyacetylene. The cells were then collected and washed with PBS (twice) and the assay plate incubated for 30 min at room temperature. The cleavage of substrate Z-DEVD-pNa for caspase-3 activity was quantified by measurement of absorbance at 405 nm on a spectrophotometric microplate reader.

Damage index

Nuclear damage to the DNA in the bone marrow cells was assessed by means of the comet assay method, according to Singh *et al*.[31] with some modifications.[32] The slides were first coated with a 1% normal agarose layer. Next, approximately 2×10^4 cells were suspended in 50 μL of 1.0% low melting point agarose and layered onto the slides, which were immediately covered with cover slips. After agarose solidification at 4 °C for 5 min, the cover slips were removed and the slides were treated with polyacetylene **1** at 54.3 μmol L^{-1} for 1 hour. Afterwards, the slides were washed with cold PBS (three times), and immersed for 1 h at 4 °C in fresh lysis solution (2.5 mol L^{-1} NaCl, 100 mmol L^{-1} Na_2 EDTA, 10 mmol L^{-1} Tris, 1% sodium lauryl sarcosinate, pH 10) containing 1% Triton X-100 and 10% of DMSO. The slides were equilibrated in alkaline solution (1 mmol L^{-1} Na_2 EDTA, 300 mmol L^{-1} NaOH, pH 10) for 30 min. Electrophoresis was carried out for 30 min at 25 V, 300 mmol L^{-1}. Afterwards, the slides were then neutralized by washing three times with 0.4 mol L^{-1} Tris buffer (pH 7.5) at 5 min intervals. The slides were then stained with ethidium bromide (20 μg mL^{-1}). The images were scored using a fluorescent microscope (Olympus CKX41SF2/CKX41-RFA equipped with a 510-569 nm excitation filter). Based on the extent of strand breakage, the cells were classified, according to their tail length, in five levels, ranging from 0 (no visible tail) to 4 (head of comet still detectable, but most of the DNA in the tail).[33] Comparative damage was performed by measurement of the damage index using the equation: Σ (Level 0 x 0) + (Level 1 x 1) + (Level 2 x 2) + (Level 3 x 3) + (Level 4 x 4), with a maximum score of 100.[34]

Statistical analysis

The results are expressed as mean values ± SD from three separated experiments. The IC_{50} values, *i.e.*, the concentration necessary for 50% inhibition, were calculated from the dose response curves using linear regression analysis that give a percentage of inhibition values. Group differences were determined by analysis of variance (ANOVA). When statistically significant differences were indicated by ANOVA, the values were compared by the

Tukey test. The differences were considered statistically significant from the controls at $p < 0.05$.

Acknowledgments

The authors are grateful to Prof. Dr. Q. B. Cass and Dr. J. C. Barreiro of the Federal University of São Carlos, Brazil, for the ESIMS and ESI-MS/MS analysis and Dr. A. C. Araújo of the University of Vale do Itajaí for the botanical identification of plant material, as well as to CAPES, CNPq and FINEP for its financial support and fellowships.

Supplementary Information

Supplementary information containing 1D and 2D NMR, MS, IR and UV data is available free of charge at http://jbcs.org.br, as a PFF file.

References

1. Bohlmann, F.; Jakupovic, J.; Gupta, R. K.; King, R. M.; Robinson, H.; *Phytochemistry* **1981**, *20*, 473.
2. Bohlmann, F.; Zdero, C.; King, R. M.; Robinson, H.; *Phytochemistry* **1982**, *21*, 695.
3. Kuo, Y. H.; Kuo, Y. J.; Yu, A. S.; Wu, M. D.; Ong, C. W.; Yang, L. M.; Huang, J. T.; Chen, C. F.; Li, S. Y.; *Chem. Pharm. Bull.* **2003**, *51*, 425.
4. Koul, J. L.; Koul, S.; Singh, C.; Taneja, S. C.; Shanmugavel, M.; Kampasi, H.; Saxena, A. K.; Qazi, G. N.; *Planta Med.* **2003**, *69*, 164.
5. Jisaka, M.; Ohigashi, H.; Takegawa, K.; Huffman, M. A.; Koshimizu, K.; *Biosci. Biotechnol. Biochem*. **1993**, *57*, 833.
6. Izevbigie, E. B.; Bryant, J. L.; Walker, A.; *Exp. Biol. Med.* **2004**, *229*, 163.
7. Nergard, C. S.; Diallo, D.; Michaelsen, T. E.; Malterud, K. E.; Kiyohara, H.; Matsumoto, T.; Yamada, H.; Paulsen, B. S.; *J. Ethnopharmacol.* **2004**, *91*, 141.
8. Lambertini, E.; Piva, R.; Khan, M. T.; Lampronti, I.; Bianchi, N.; Borgatti, M.; Gambari, R.; *Int. J. Oncol.* **2004**, *24*, 419.
9. Cabrera, A. L.; Klein, R. M.; *Fl. Ilustr. Catarin.* **1980**, 354.
10. Freire, M. F. I.; Abreu, H. S.; Cruz, L. C. H.; Freire, R. B.; *Braz. J. Microbiol.* **1996**, *27*, 1.
11. Leite, S. N.; Palhano, G.; Almeida, S.; Biavatti, M. W.; *Fitoterapia* **2002**, *73*, 496.
12. Pagno, T; Blind, L. Z; Biavatti, M. W; Kreuger, M. R. O.; *Braz. J. Med. Biol. Res*. **2006**, *39*, 1483.
13. Hearn, M. T. W.; Turner, J. L.; *J. Chem. Soc., Perkin Trans. 2* **1976**, 1027.
14. Muller, N.; Pritchard, D. E.; *J. Chem. Phys.* **1959**, *31*, 768.
15. Muller, N.; Pritchard, D. E.; *J. Chem. Phys.* **1959**, *31*, 1471.
16. Höbold, W.; Radeglia, R.; Klose, D.; *J. Prakt. Chem.* **1976**, *318*, 519.
17. Guillet, G.; Philogene, B. J. R.; O'Meara, J.; Durst, T.; Arnason, J. T.; *Phytochemistry* **1997**, *46*, 495.
18. Satoh, A.; Narita, E.; Nishimura, H.; *Biosci., Biotechnol., Biochem.* **1996**, *60*, 152.
19. Yamazoe, S.; Hasegawa, K.; Shigemori, H.; *Phytochemistry* **2007**, *68*, 1706.
20. Chobot, V.; Buchta,V.; Jahodarova, H.; Pour, M.; Opletal, L.; Jahodar L.; Harant, P.; *Fitoterapia* **2003**, *74*, 288.
21. Hadacek, F.; Greger, H.; *Phytochem. Anal.* **2000**, *11*, 137.
22. Constabel, C.P.; Towers, G.H.N.; *Planta Med.* **1989**, *55*, 35.
23. Towers, G.H.N.; Abramowski, Z.; Finlayson, A.J.; Zucconi, A.; *Planta Med.* **1985**, *51*, 225.
24. Jahodář, L.; Klečáková, J.; *Chem. Listy* **1999**, *93*, 320.
25. Ebermann, R.; Alth, G.; Kreitner, M.; Kubin, A.; *J. Photochem. Photobiol. B* **1996**, *36*, 95.
26. Pellati, F.; Calo, S.; Benvenuti, S.; Adinolfi B.; Nieri P.; Melegari, M.; *Phytochemistry* **2006**, *67*, 1359.
27. Mosmann, T.; *J. Immunol. Methods* **1983**, *65*, 55.
28. Choi, H. J.; Yee, S. B.; Park, S. E.; Im, E.; Jung, J. H.; Chung, H. Y.; Choi, Y. H.; Kim, N. D.; *Cancer Lett.* **2006**, *232*, 214.
29. Salvesen, G. S.; Dixit, V. M.; *Cell* **1997**, *91*, 443.
30. Cruz-Chamorro, L.; Puertollano, M. A.; Puertollano, E.; Cienfuegos, G. A.; Pablo, M. A.; *Peptides* **2006**, *27*, 1201.
31. Singh, S.; Lowe, D. G.; Thorpe, D. S.; Rodriguez, H.; Kuang, W. J.; Dangott, L. J.; Chinkers, M.; Goeddel, D. V.; Garbers, D. L.; *Nature* **1988**, *334*, 708.
32. Collins, A. R.; Dusinska, M. In *Methods in Molecular Biology*; Armstrong, D., ed.; Humana Press: NJ, 2002, vol. 186.
33. Cavalcanti, B. C.; Costa-Lotufo, L. V.; Moraes, M. O.; Burbano, R. R.; Silveira, E. R.; Cunha, K. M.; Rao, V. S.; Moura, D. J.; Rosa, R. M.; Henriques, J. A.; Pessoa, C.; *Food Chem. Toxicol.* **2006**, *44*, 388.
34. Liu, W.; Christenson, S.; Standage, S.; Shen, B.; *Science* **2002**, *297*, 1170.

Received: July 3, 2008
Web Release Date: July 6, 2009

FAPESP helped in meeting the publication costs of this article.

J. Braz. Chem. Soc., Vol. 20, No. 7, S1-S10, 2009.
Printed in Brazil - ©2009 Sociedade Brasileira de Química
0103 - 5053 $6.00+0.00

A New Polyacetylene from *Vernonia scorpioides* (Lam.) Pers. (Asteraceae) and its *in vitro* Antitumoral Activity

Humberto Buskuhl,[a] Rilton A. Freitas,[a] Franco Delle Monache,[b] Andersson Barison,[c] Francinete R. Campos,[c] Yuri E. Corilo,[d] Marcos N. Eberlin[d] and Maique W. Biavatti*[,a,#]

[a]*Centro de Ciências da Saúde, Universidade do Vale do Itajaí, 88302-202 Itajaí-SC, Brazil*

[b]*Dipartimento di Chimica e Tecnologia delle Sostanze Biologicamente Attive, Università "La Sapienza", Roma, Italy*

[c]*Departamento de Química, Centro Politécnico, Universidade Federal do Paraná, 81530-900 Curitiba-PR, Brazil*

[d]*Instituto de Química, Universidade Estadual de Campinas, 13083-970 Campinas-SP, Brazil*

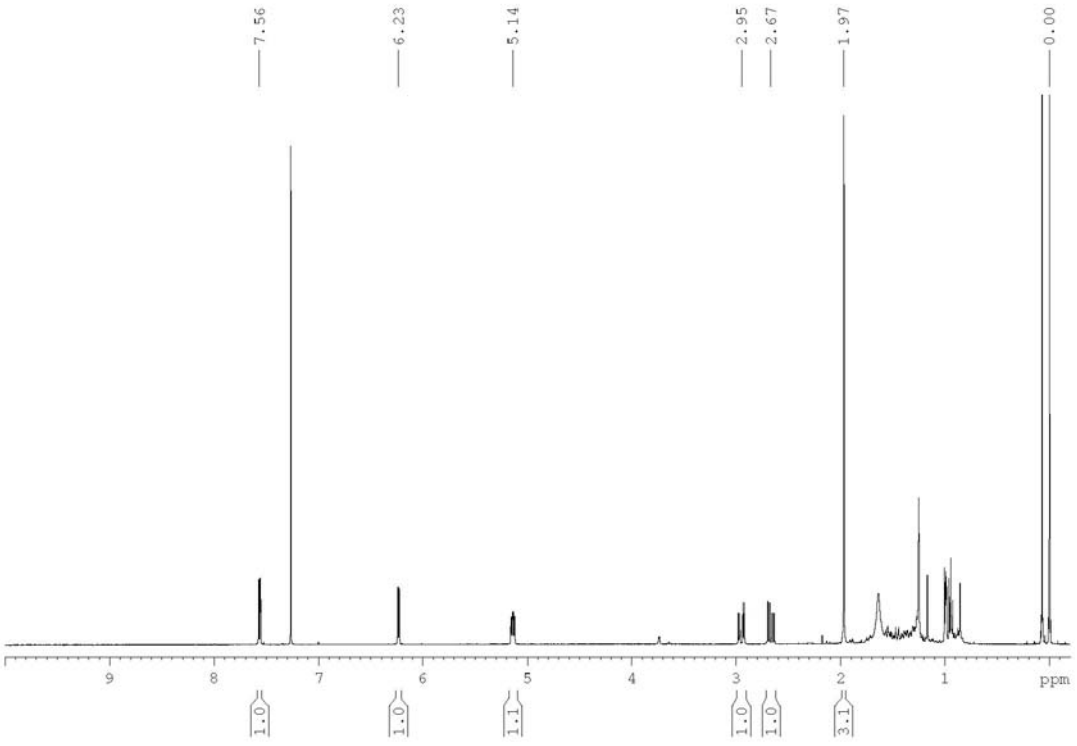

Figure S1. ^{1}H NMR spectrum of the polyacetylene (**1**) in $CDCl_3$ at 400 MHz.

*e-mail: maique@ccs.ufsc.br
[#] Present address: Laboratório de Farmacognosia, Departamento de Ciências Farmacêuticas, Centro de Ciências da Saúde, Universidade Federal de Santa Catarina, Trindade, 88040-900 Florianopolis-SC, Brazil

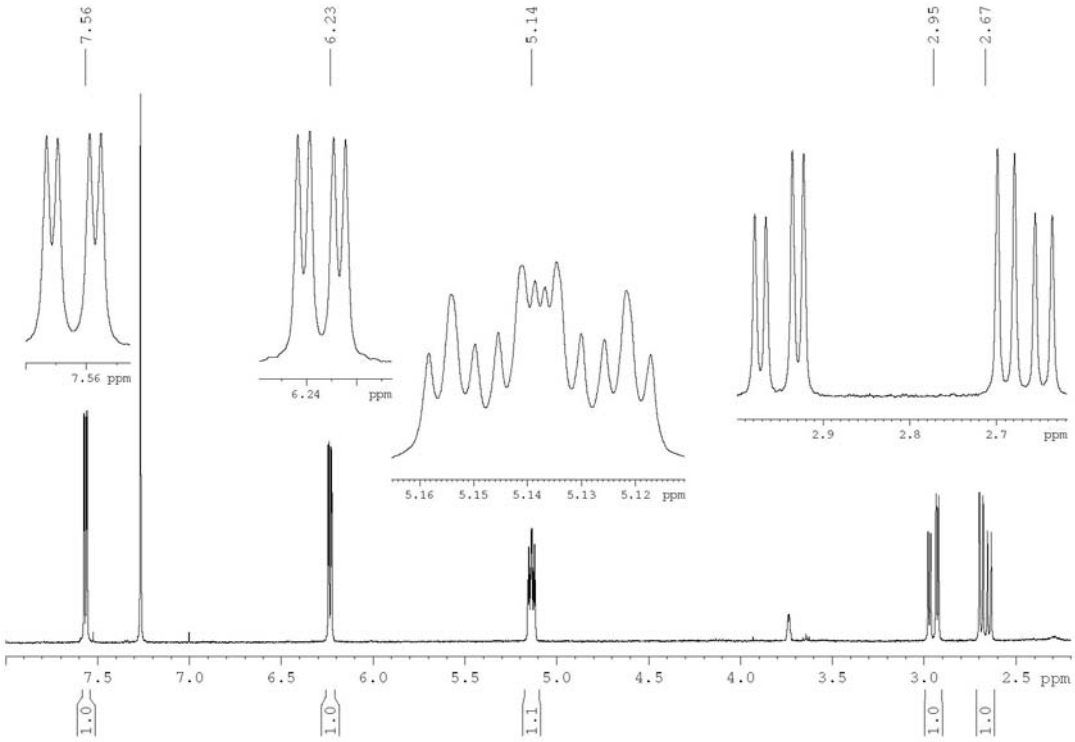

Figure S2. Expansions of the ^{1}H NMR spectrum of the polyacetylene (**1**) in $CDCl_3$ at 400 MHz.

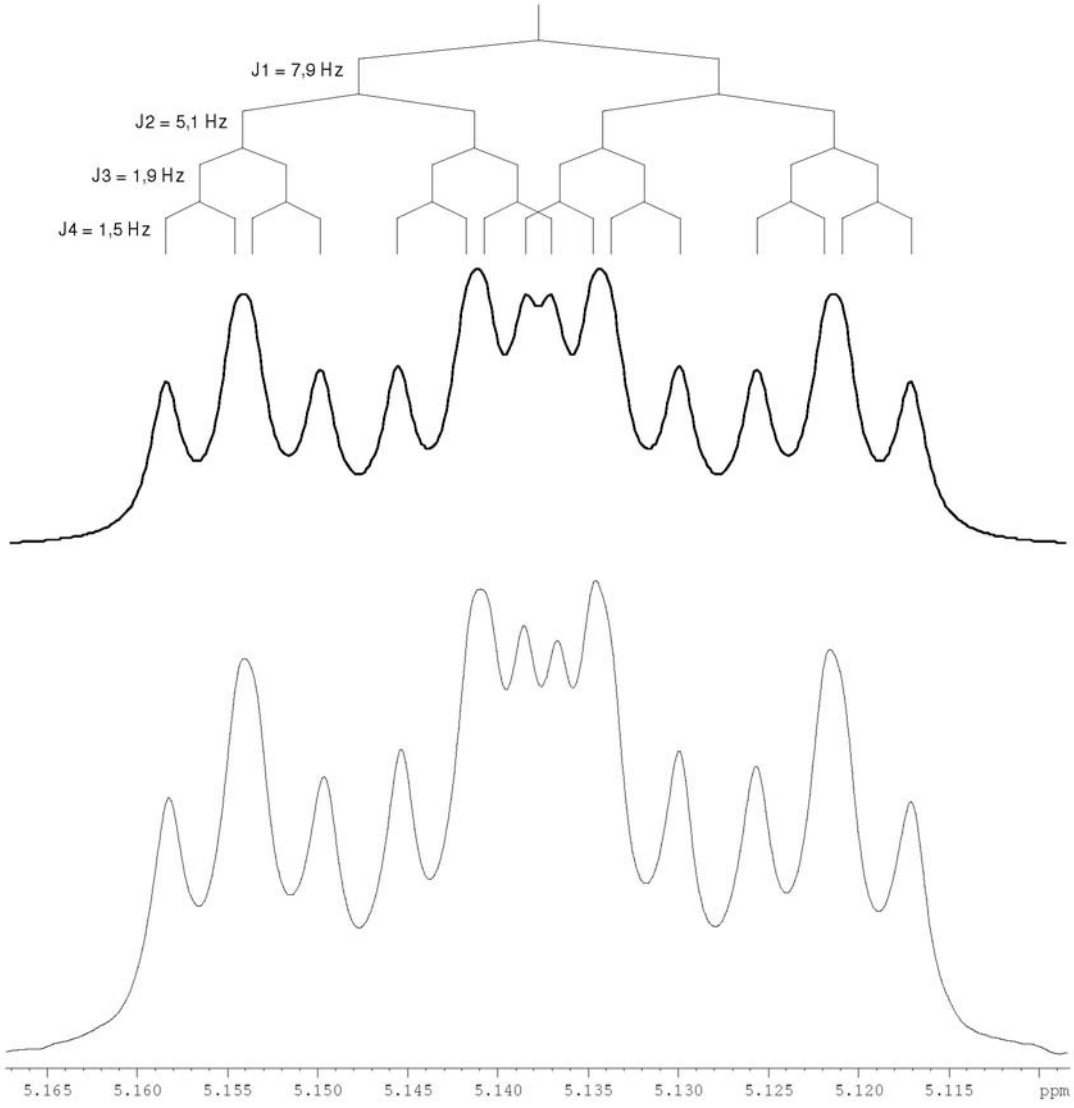

Figure S3. Simulated (Top) and experimental (Bottom, $CDCl_3$ at 400 MHz) ^1H NMR signal in order to understand the multiplicity of H-5 at 5.14 ppm (*dddd* 7.9, 5.1, 1.9, 1.5) of the polyacetylene (**1**). The signal was simulated with aid of the FOMSC-3 software (http://artemis.ffclrp.usp.br/NMR.htm).

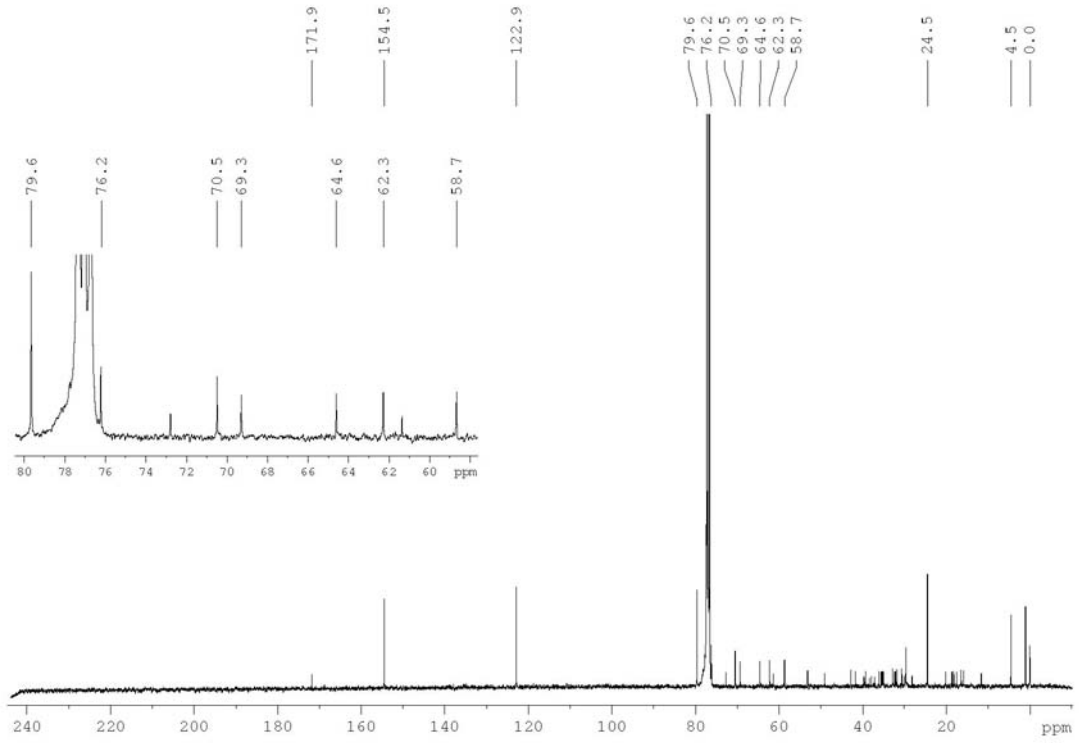

Figure S4. $^{13}C\{^{1}H\}$ NMR spectrum of the polyacetylene (**1**) in $CDCl_3$ at 100 MHz. Insert is an expansion showing the signal from C-2' to C-7'.

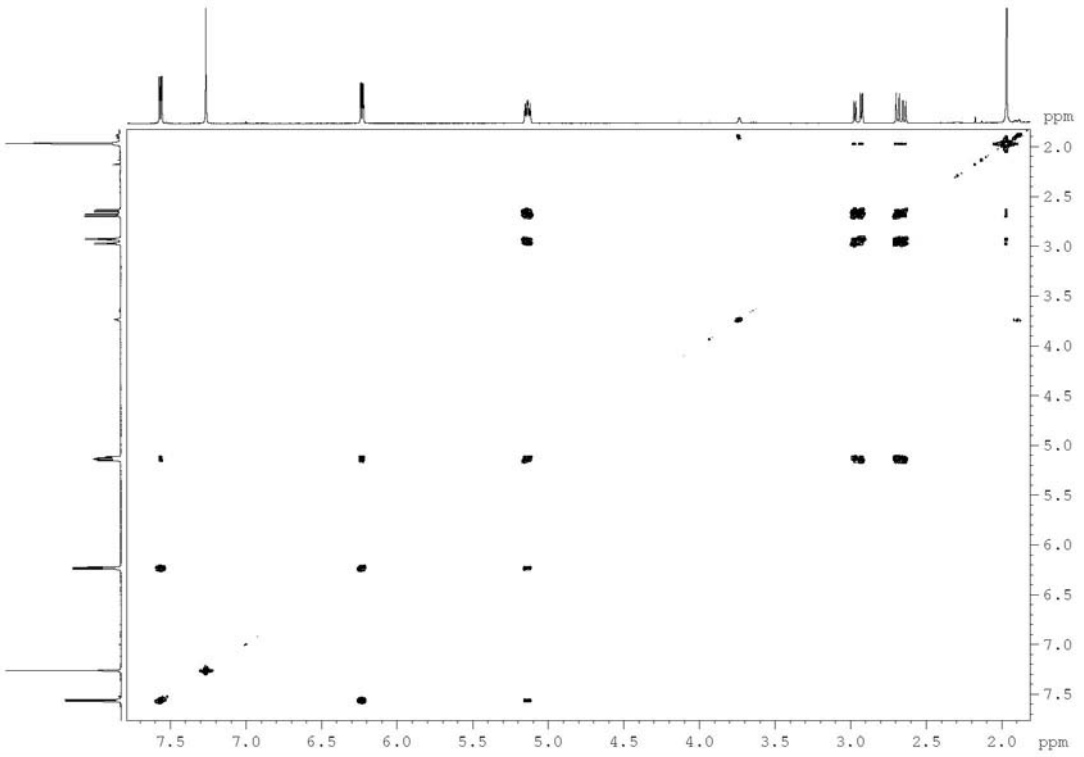

Figure S5. ^{1}H-^{1}H correlation map from COSY NMR experiment of the polyacetylene (**1**) in $CDCl_3$ at 400 MHz.

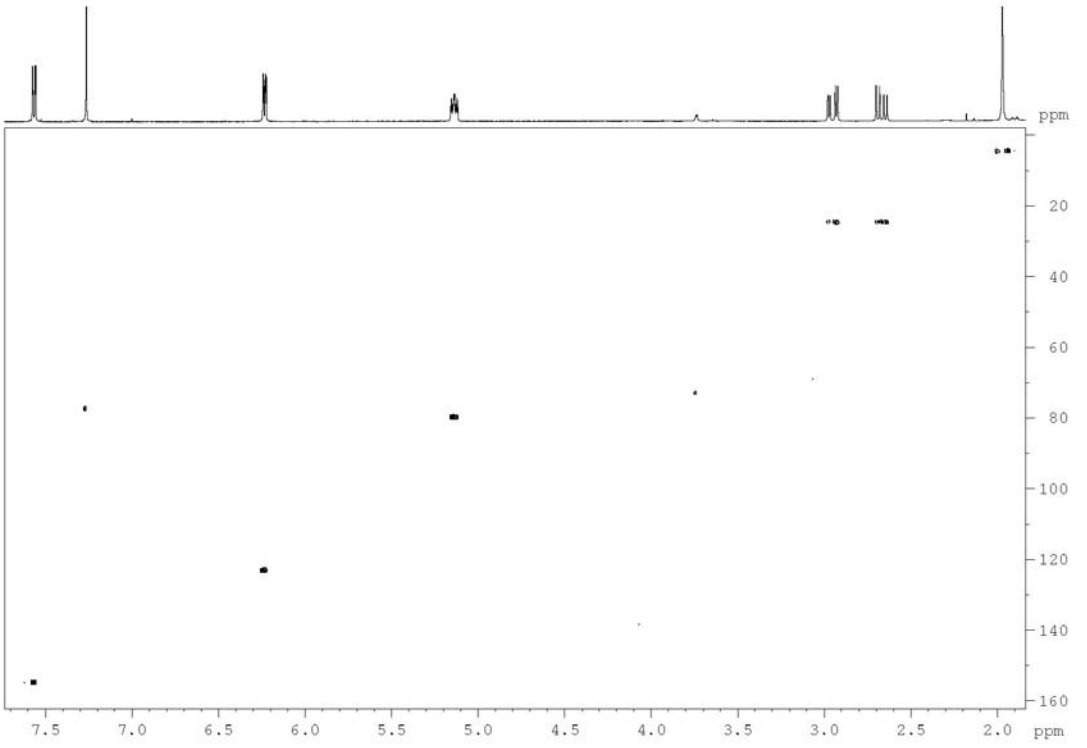

Figure S6. ^{1}H-^{13}C one-bond correlation map from HSQC NMR experiment of the polyacetylene (**1**) in $CDCl_3$ at 400 and 100 MHz.

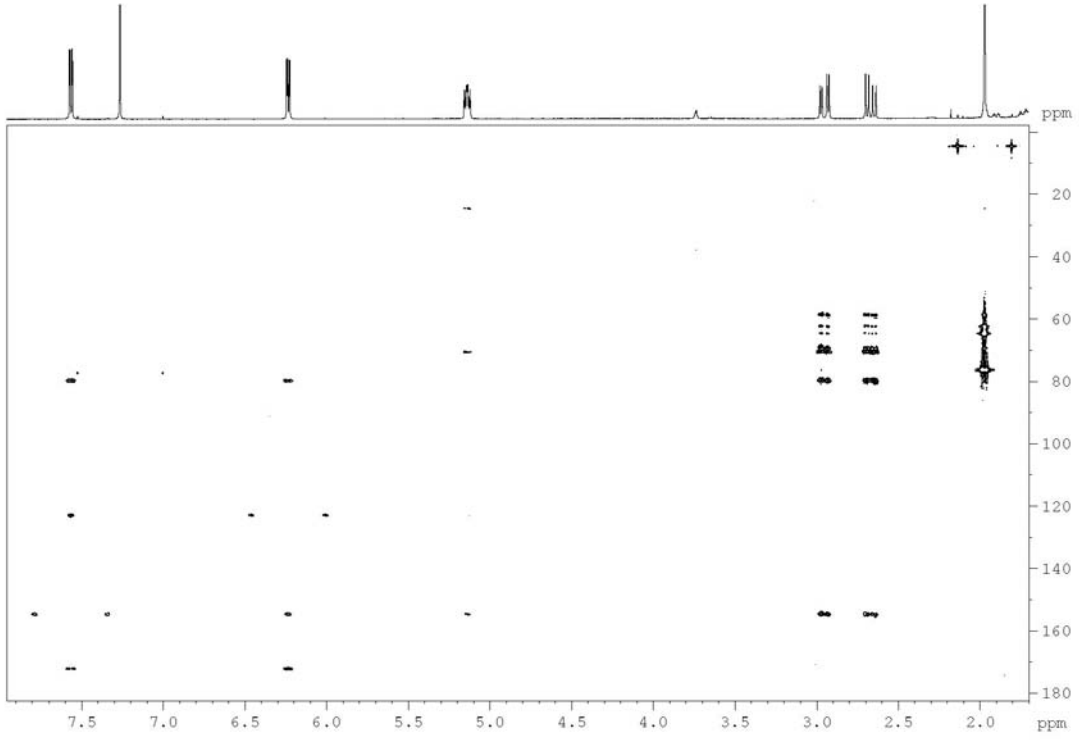

Figure S7. ^{1}H-^{13}C long-range correlation map from HMBC NMR experiment of the polyacetylene (**1**) in $CDCl_3$ at 400 and 100 MHz.

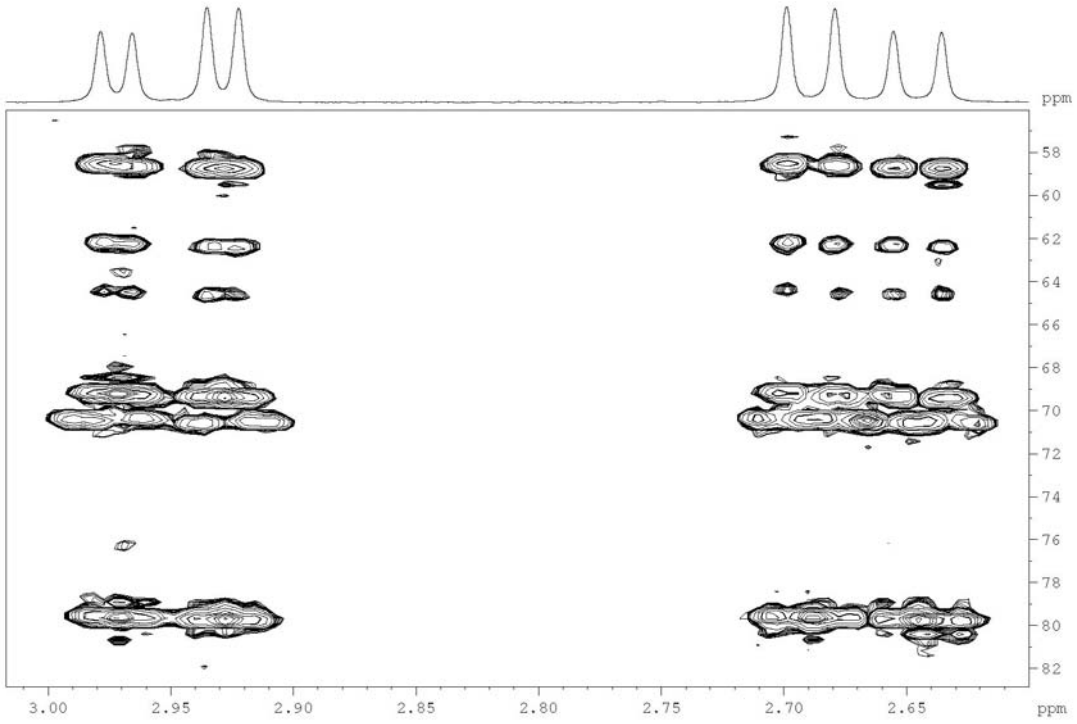

Figure S8. Expansion of the ^{1}H-^{13}C long-range correlation map from HMBC NMR experiment of the polyacetylene (**1**) in $CDCl_3$ at 400 and 100 MHz, showing the correlations for both H-1' at 2.67 and 2.95 ppm.

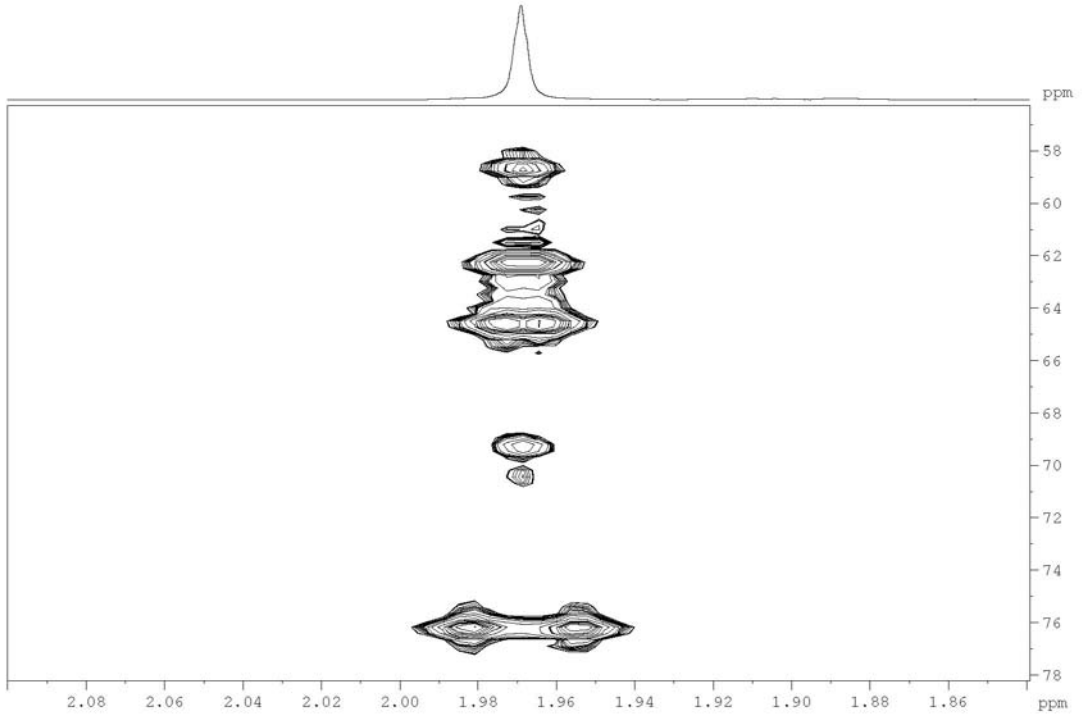

Figure S9. Expansion of the ^{1}H-^{13}C long-range correlation map from HMBC NMR experiment of the polyacetylene (**1**) in $CDCl_3$ at 400 and 100 MHz, showing the correlations for H-8' at 2.97 ppm.

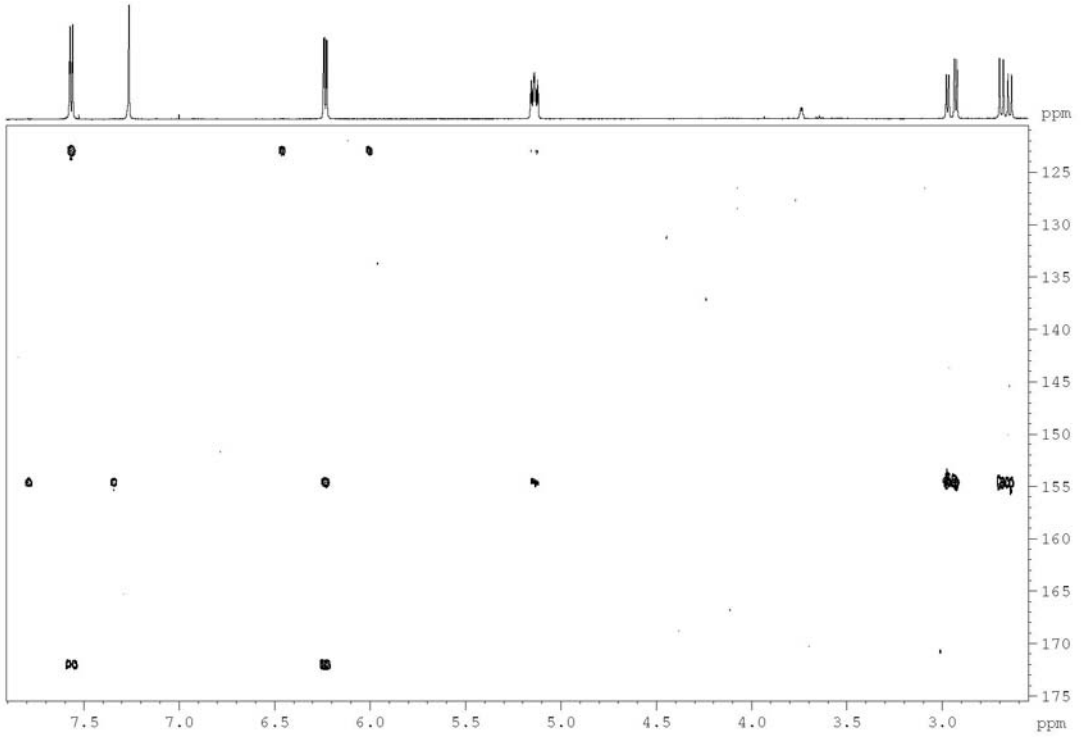

Figure S10. Expansion of the ^{1}H-^{13}C long-range correlation map from HMBC NMR experiment of the polyacetylene (**1**) in $CDCl_3$ at 400 and 100 MHz, showing the correlations with the olefinic C-2 and C-3 and the carbonyl C-4.

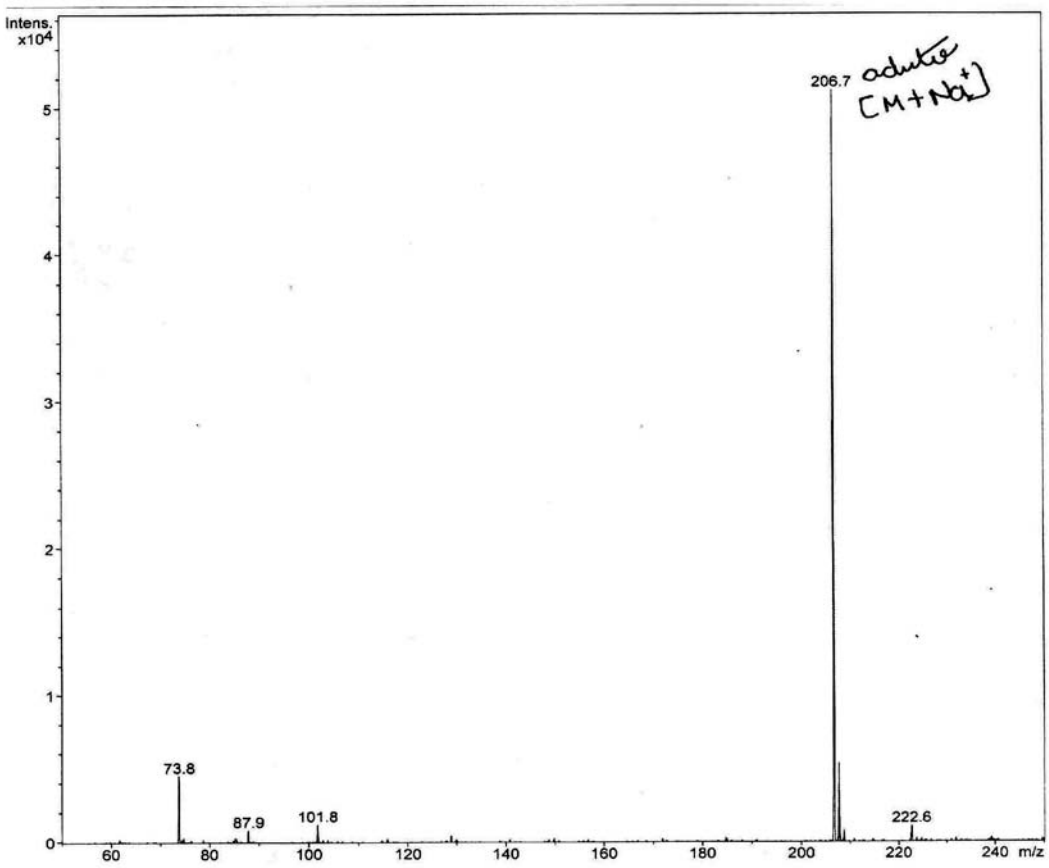

Figure S11. ESI-MS of the polyacetylene (**1**) in MeOH, positive mode.

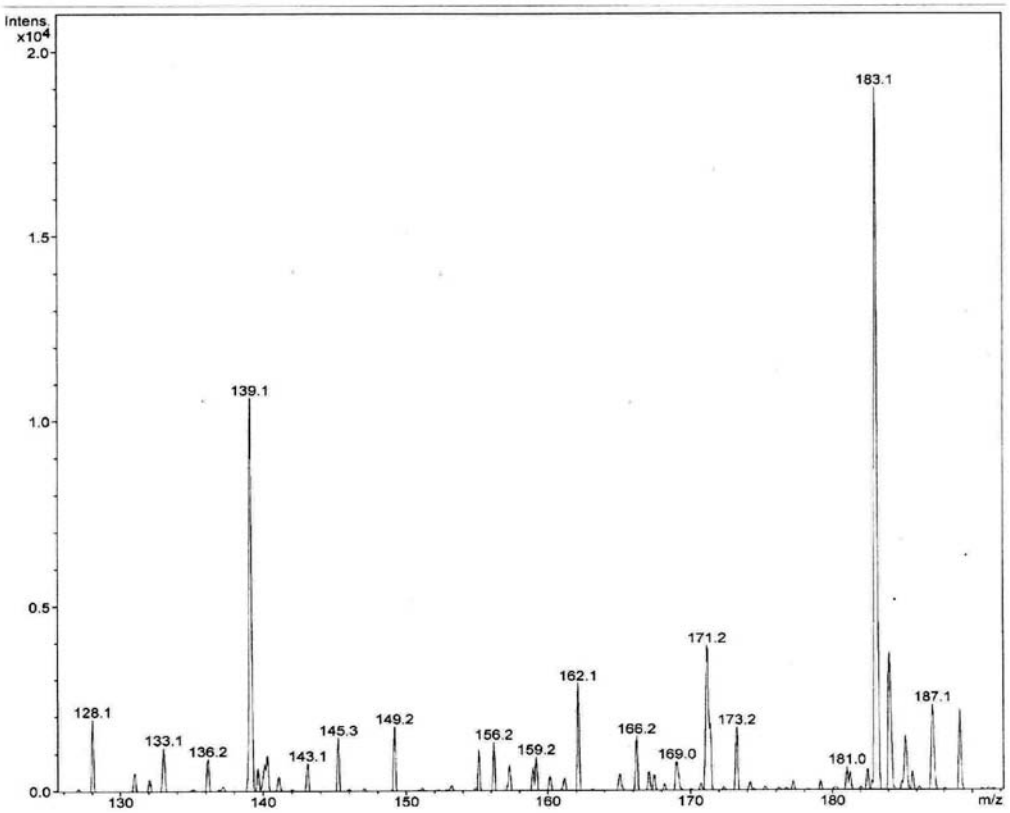

Figure S12. ESI-MS of the polyacetylene (**1**) in MeOH, negative mode.

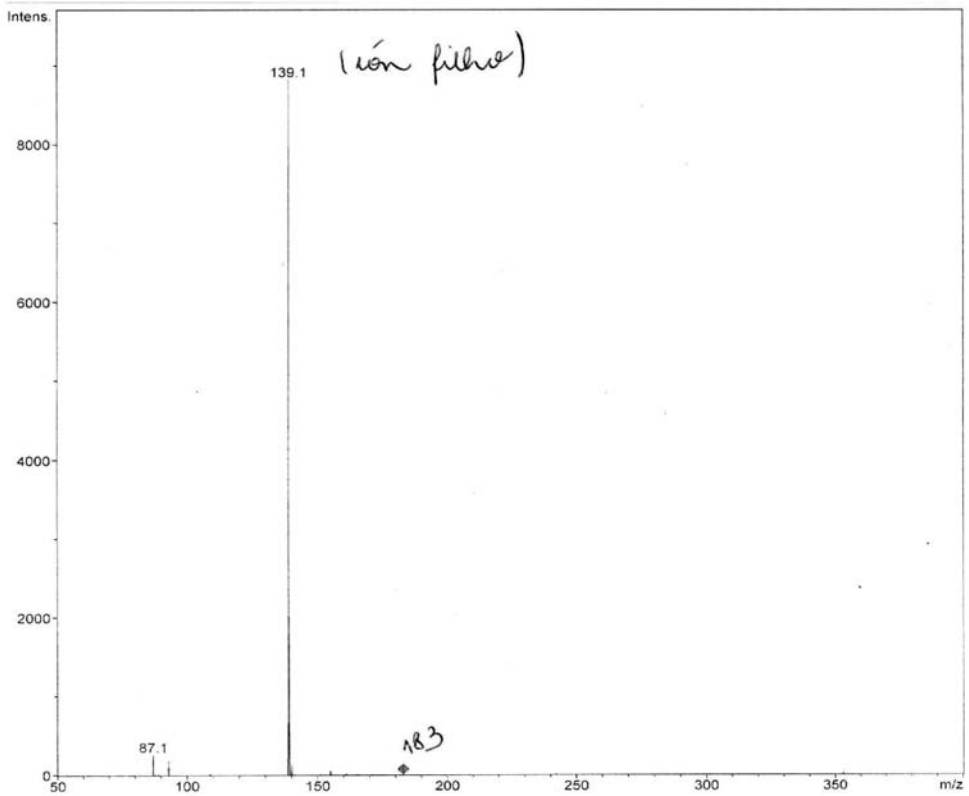

Figure S13. ESI-MS/MS of the polyacetylene (**1**) in MeOH, negative mode at 40 eV.

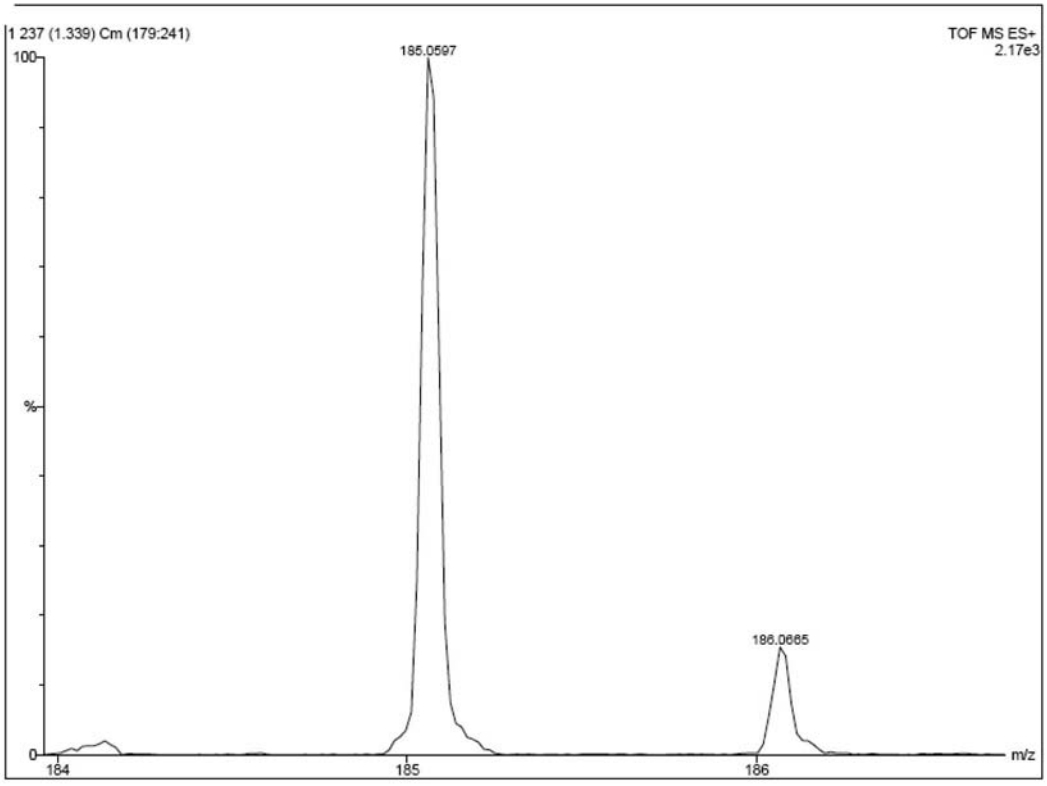

Figure S14. HR-ESI-TOF-MS of the polyacetylene (**1**), positive mode.

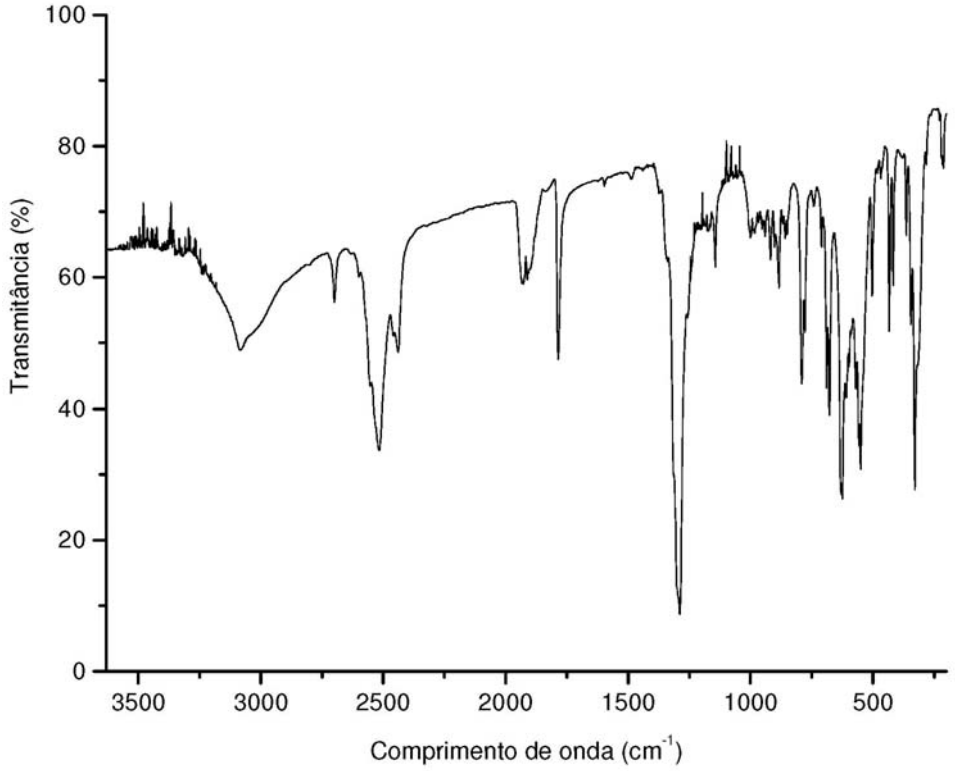

Figure S15. FT-IR spectrum of the polyacetylene (**1**) in KBr pellets.

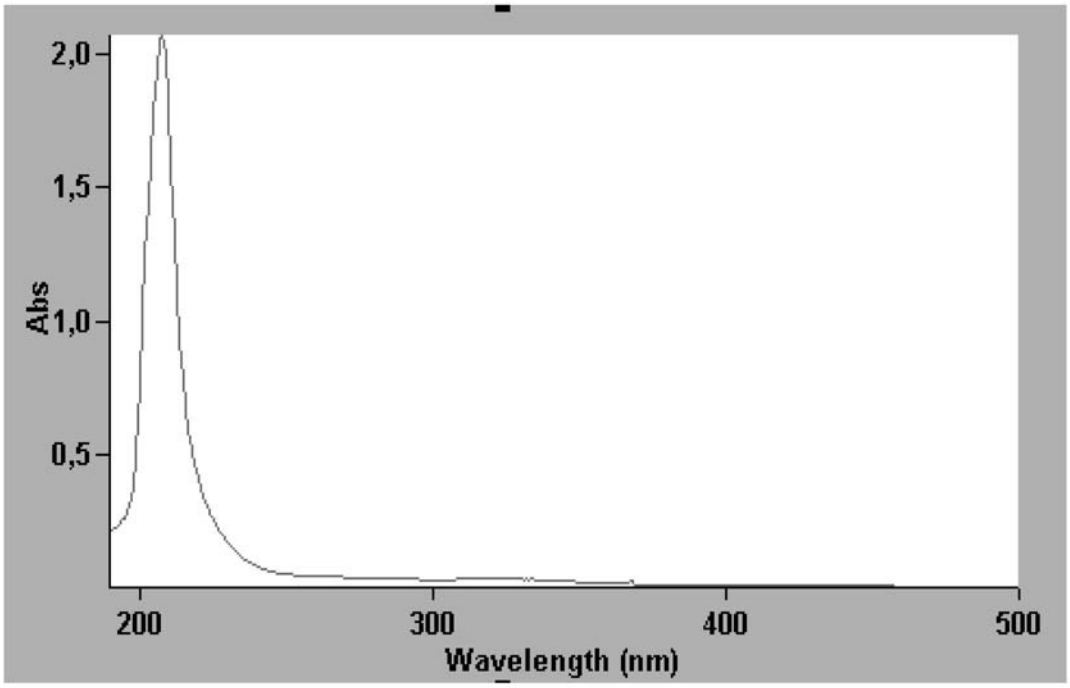

Figure S16. UV spectrum of the polyacetylene (**1**) in MeOH.